J. Membrane Biol. 121, 79–90 (1991)
002226319100058K

The Journal of
Membrane Biology

Na^+ Channel Activity in Cultured Renal (A6) Epithelium: Regulation by Solution Osmolarity

N.K. Wills, L.P. Millinoff, and W.E. Crowe
Department of Physiology and Biophysics, University of Texas Medical Branch, Galveston, Texas 77550

Summary. Solution osmolarity is known to affect Na^+ transport rates across tight epithelia but this variable has been relatively ignored in studies of cultured renal epithelia. Using electrophysiological methods to study A6 epithelial monolayers, we observed a marked effect of solution tonicity on amiloride-sensitive Na^+ currents (I_{sc}). I_{sc} for tissues bathed in symmetrical hyposmotic (170 mOsm), isosmotic (200 mOsm), and hyperosmotic (230 or 290 mOsm) NaCl Ringer's solutions averaged 25 ± 2, 9 ± 2, 3 ± 0.4, and 0.6 ± 0.5 $\mu A/cm^2$, respectively. Similar results were obtained following changes in the serosal tonicity; mucosal changes did not significantly affect I_{sc}. The changes in I_{sc} were slow and reached steady-state within 30 min. Current fluctuation analysis measurements indicated that single-channel currents and Na^+ channel blocker kinetics were similar for isosmotic and hyposmotic conditions. However, the number of conducting Na^+ channels was approximately threefold higher for tissues bathed in hyposmotic solutions. No channel activity was detected during hyperosmotic conditions. The results suggest that Na^+ channels in A6 epithelia are highly sensitive to relatively small changes in serosal solution tonicity. Consequently, osmotic effects may partly account for the large variability in Na^+ transport rates for A6 epithelia reported in the literature.

Key Words A6 · epithelium · Na^+ channel · current fluctuation analysis · CDPC · amiloride · osmolarity

Introduction

Many cells demonstrate volume-related regulation of ion transport processes when exposed to anisosmotic media (*cf.* Hoffman & Simonsen, 1989). It has long been recognized that solution osmolarity can have important effects on transepithelial Na^+ transport across so-called tight epithelia. In studies of the isolated frog skin, Ussing (1965) demonstrated that hyperosmotic serosal solutions decreased Na^+ transport (as measured by amiloride-sensitive short-circuit current, I_{sc}) and caused cell shrinkage (measured as a decrease in tissue height). Conversely, hypotonic serosal solutions resulted in increased I_{sc} and cell swelling.

The mechanism of these changes in Na^+ transport remains poorly understood. One problem is the complex structure of most epithelia. For example, the frog skin contains a layer of underlying connective tissue and is composed of different cell types. Nonetheless, recent studies of a number of other epithelia have clearly shown that hyperosmotic solutions result in a decrease in basolateral membrane K^+ conductance (*cf.* Lewis & Donaldson, 1990). Because of the more simple monolayer structure of cultured renal epithelia and the ability to precisely control the extracellular environment, we sought to determine whether similar effects of solution osmolarity on I_{sc} could be detected in cultured renal A6 epithelium.

A6 cells have Na^+ transport properties that are similar to renal distal tubule cells and have recently become a popular model for studies of Na^+ transport regulation. Under normal conditions, I_{sc} across this epithelium is due to conductive, amiloride-sensitive Na^+ transport that is stimulated by several hormones, including aldosterone, vasopressin (Perkins & Handler, 1981) and insulin (Fidelman et al., 1982). We now report a potent regulation of Na^+ transport in this tissue by serosal solution osmolarity. Small (15%) perturbations in solution osmolarity led to threefold changes in I_{sc}. Moreover, these alterations were fully accounted for by changes in the number of conducting apical membrane Na^+ channels.

Materials and Methods

Cell Culture

A6 (*Xenopus laevis*) renal cells obtained from American Type Culture Collection (Bethesda, MD) were grown on permeable supports according to previously described methods (Wills & Millinoff, 1990). Briefly, cells at passages 74–79 were seeded onto

permeable filter paper supports (Millicell-HA, 0.4-μm pore, 30-mm diameter, Millipore, Bedford, MA) at a seeding density of 10^6 cells per well (i.e., 2×10^5 cells/cm^2). The cells were fed three times weekly with a Dulbecco's Modified Eagle's Medium (amphibian formula; Gibco Laboratories, Grand Island, NY, catalogue no. 84-5022) which was supplemented with antibiotics and 10% fetal calf serum (Hyclone Laboratories, Logan, UT). The solution osmolarity was measured using a vapor pressure osmometer (Model 5500, Wescor, Logan UT). The measured osmolarity was 200 mOsm, which was defined as isosmotic.

Experimental Chambers and Bathing Solutions

Chambers

After 12–14 days of incubation, the epithelial monolayers were mounted in an Ussing chamber designed to eliminate edge damage (Lewis, 1977; chamber opening = 1 or 4.2 cm^2). The epithelium was bathed on both sides with a NaCl-HCO_3 Ringer's solution that was continuously stirred and bubbled with air containing 1% CO_2. Solution temperature was maintained at 28°C by water jackets surrounding the chambers.

Solutions

The electrolyte composition of the bathing solution was designed to match the culture medium and contained (in mM): 74.4 NaCl, 5.4 KCl, 8 $NaHCO_3$, 1.4 $CaCl_2$, 1.7 $MgSO_4$, 0.9 NaH_2PO_4, 5.5 glucose, 1 Na pyruvate, and 1 N-2-hydroxyethylpiperazine-N'-2-ethanesulfonic acid (HEPES). The osmolarity of this solution was 170 mOsm, and the pH was maintained at 7.4 by bubbling the solution (*see above*). Isotonic or hypertonic solutions were made by adding the appropriate amounts of either mannitol or NaCl. Amiloride (a gift of Merck, Sharp, and Dohme) and 6-chloro-3,5'-diaminopyrazine-2-carboxamide (CDPC, Aldrich Chemical, Milwaukee, WI) were prepared as concentrated stock solutions in NaCl Ringer's solution, and microliter aliquots were added to the bathing solutions to achieve the specified concentrations.

Electrical Measurements

Transepithelial DC Measurements

Methods for measuring transepithelial current and voltage were similar to those described previously (Wills & Millinoff, 1990). Briefly, the transepithelial voltage (V_T) and current (I) were monitored using pairs of Ag-AgCl wires or 1 M NaCl agar bridges connected to Ag-AgCl wires led to an automatic voltage clamp. Currents were read to ± 0.1 μA/cm^2 accuracy using a digital meter and a computer A/D system. In current fluctuation analysis experiments, the size of the chamber opening area was reduced from 4.2 to 1 cm^2 to avoid saturation of the voltage-clamp amplifiers. Transepithelial electrical properties normalized to membrane area were identical for the two nominal chamber areas.

Current Fluctuation Analysis

Current fluctuation analysis methods were similar to those previously described (Wills et al., 1984) and used an ultra-low noise voltage clamp (Van Driessche & Lindemann, 1978). The tissue was continuously short-circuited except for brief periods in which the open-circuit potential was measured. The I_{sc} signal was led to a high-pass RC filter (0.5 Hz), amplified and then fed into a low-pass filter (120 dB/octave; model LP120; Unigon Instruments, White Plains, NY). The resulting noise signal was digitized using a 12-bit A/D converter and laboratory computer system (LSI 11/73; Indec Systems, Sunnyvale, CA). The sampling rate was 1 msec/point resulting in 81,920 sequential data points. These data were divided into blocks of 512 points, and each block was analyzed using a fast Fourier transform program. This resulted in 160 power-density spectra that were averaged to provide a final mean spectrum.

To analyze the mean spectrum, the data were reduced to 50–100 points that were logarithmically spaced over the frequency range. A Lorentzian function was fit to the power density spectrum (PDS) using a nonlinear least-squares curve fitting routine (N-Fit, Island Products, Galveston, TX). In most cases it was necessary to use a function that takes into account $1/f$ noise at low frequencies (Van Driessche & Zeiske, 1980) as follows:

$$S(f) = B/f^b + S_o/[1 + (f/f_c)^2] \quad (1)$$

where S_o is the low frequency plateau value, f_c is the corner frequency, and B/f^b is the low frequency $1/f$ noise. S_o and f_c values were used to calculate the single-channel current (i) and channel density (M) as follows (*see also* Wills et al., 1984):

$$i = S_o(k_{on}[\text{CDPC}] + k_{off})^2/(k_{on}[B]4I_{Na}) \quad (2)$$

$$M = I_{Na}/iP_o \quad (3)$$

where the parameters f_c and S_o are as defined above, $[B]$ is blocker concentration, k_{on} and k_{off} are the apparent association rate constant and the dissociation rate constant, and I_{Na} is the remaining portion of the blocker-sensitive current. P_o is defined as the probability that the channel is open and is calculated as $1 - k_{on}[\text{CDPC}]/(k_{on}[\text{CDPC}] + k_{off})$ or $1 - P_c$, the probability that the channel is closed (for discussion, *see* Krattenmacher et al., 1988).

Equivalent Circuit Analysis

Paracellular resistance (R_j) or its reciprocal, paracellular conductance (G_j), was assessed using methods described by Wills and Millinoff (1990). Briefly, tight junctional resistance (R_j) and cellular electromotive force (E_c) were calculated from the R_T and V_T measurements during amiloride action. A plot of V_T versus R_T yields a linear double intercept plot as follows (Wills, Lewis & Eaton, 1979):

$$1 = V_T/E_c + R_T/R_j \quad (4)$$

where E_c is the cellular electromotive force (E_c) and R_j is the paracellular resistance. Cellular resistance ($1/G_c$) was calculated as $(G_T - G_j)^{-1}$.

Results

As a first step in characterizing the effects of solution osmolarity on epithelial electrical properties, solution osmolarity was changed symmetrically (i.e., on both sides of the epithelium) and the time course of

changes in transepithelial short-circuit current (I_{sc}) and conductance (G_T) was measured. Next, unilateral solution replacements were performed to assess the sideness of these effects. In addition, the Na^+ channel blocker amiloride was applied to the mucosal bath to determine whether the changes in I_{sc} and G_T were due to alterations in conductive Na^+ transport. Equivalent circuit analysis was performed on the amiloride results to assess changes in the cellular conductance (G_c) and transcellular Na^+ driving force (E_c). Lastly, the effects of osmolarity on apical membrane Na^+ channels were determined using current fluctuation analysis and the rapid Na^+ channel blocker CDPC (Marunaka & Eaton, 1988).

Osmolarity Effects and Time Course

Symmetrical changes in solution osmolarity led to slow but marked changes in I_{sc} and G_T. In four epithelia exposed to a series of randomized bilateral solution changes, the steady-state short-circuit current (I_{sc}) in 170, 220, 230 and 290 mOsm solutions averaged 25 ± 2, 9 ± 2, 3 ± 0.4, and 0.6 ± 0.5 $\mu A/cm^2$, respectively. G_T for the same solutions averaged 468 ± 37, 341 ± 40, 307 ± 35 and 300 ± 24 $\mu S/cm^2$.

Figure 1 shows the average time course of the changes in I_{sc} observed for these experiments. Tissues were initially equilibrated in isosmotic (200 mOsm) solutions for 30 min and then changed to hyposmotic or hyperosmotic solutions at $t = 0$. (Solution changes were complete within 2 min.) In hyposmotic solutions (170 mOsm), the current slowly increased after 5–10 min, then more rapidly, and reached a new steady state level at 20–30 min. Following restoration of the control (200 mOsm) solution, I_{sc} returned to its previous level within 30 min.

When epithelia were exposed to hyperosmotic (230 or 290 mOsm) solutions, I_{sc} decreased within 5 min, reaching new steady-state levels at 20–30 min. The effects of 230 mOsm solutions were usually fully reversible upon restoration of 200 mOsm solutions, whereas I_{sc} typically showed only partial recovery from 290 mOsm solutions.

These findings demonstrate that the electrical parameters of A6 epithelium are quite sensitive to small (15%) perturbations in solution osmolarity. With the exception of 290 mOsm solutions, the alterations in I_{sc} and G_T were readily reversible. The long time course of these effects suggests that osmolarity changes do not have a direct mechanical effect (such as stretch activation of ionic channels), but rather may initiate a slow process or cascade of intracellular events.

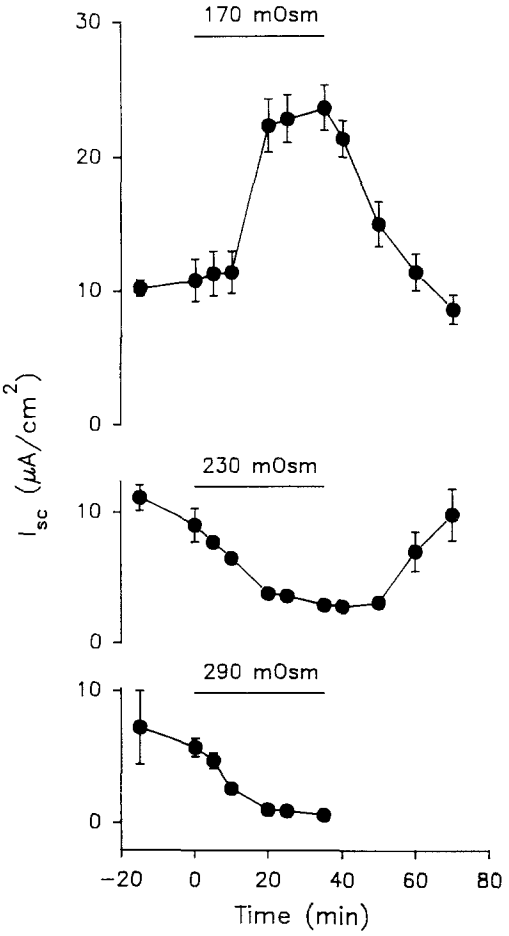

Fig. 1. Changes in transepithelial short-circuit current (I_{sc}) as a function of time after bilateral changes in solution osmolarity at time = 0. Data are averages from four tissues

Sideness of Effects

Epithelial apical (luminal) and basolateral (serosal) membranes have asymmetrical properties. Therefore, it was useful to determine which membrane mediated the osmolarity effects. Mucosal solution osmolarity had little effect on I_{sc} or G_T, although a transient increase in I_{sc} was sometimes noted for mucosal 290-mOsm solutions. As shown in Fig. 2, I_{sc} and G_T were significantly larger in 170-mOsm serosal solutions than in 200-mOsm solutions. However, these parameters did not significantly differ between tissues bathed with different mucosal solution osmolarities. Indeed, the effects of asymmetrical serosal solution osmolarity changes were essentially identical to those for symmetrical changes. The results are summarized in Figure 3 ($n = 15$). In these experiments the mucosal solution osmolarity was held constant at 200 mOsm.

In agreement with Figs. 1 and 2, both I_{sc} and G_T

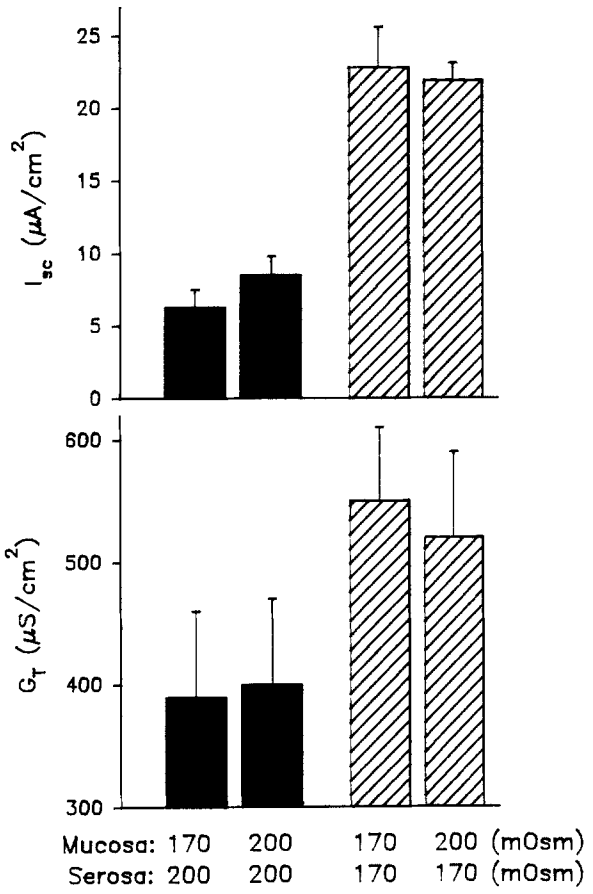

Fig. 2. Effects of solution osmolarity on transepithelial short-circuit current (I_{sc}) and conductance (G_T). Filled bars indicate 200 mOsm serosal solution and striped bars are 170 mOsm serosal solutions ($n = 4$)

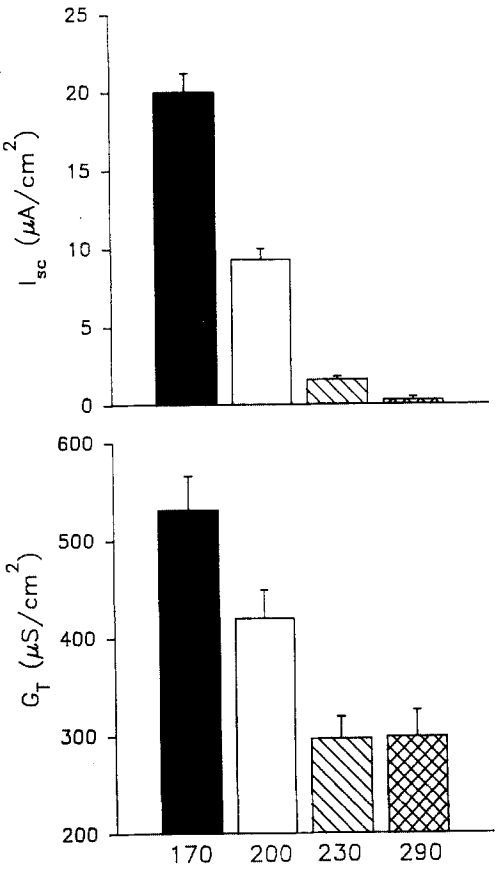

Fig. 3. Effects of different serosal solution osmolarities on I_{sc} and G_T. The osmolarity of the mucosal solution was 200 mOsm. Mean and SEM from 15 epithelia

significantly decreased as serosal solution osmolarity was increased. As in the symmetrical solution solution replacement experiments, exposure to 290 mOsm serosal solutions led to a virtual abolition of I_{sc}. These findings indicate that the effects of osmolarity originate from the serosal side of the epithelium.

To determine whether this decrease is due to osmolarity or is an unusual effect of manitol, similar symmetrical or serosal replacement studies were performed using NaCl instead of mannitol. The results were similar to those reported for mannitol: average values for I_{sc} in 170, 200, 230, and 290 mOsm solutions were 20.8 ± 2.1, 9.6 ± 1.1, 0.6 ± 0.3, and 0.3 ± 0.2 μA/cm^2, respectively ($n = 3$). G_T significantly decreased from 607 ± 66, to 516 ± 28, 439 ± 71, and 472 ± 63 μS/cm^2 (in the same order). The reason for the larger value of G_T in the 290 mOsm solution is unknown but is consistent with an epithelial chloride conductance (N.K. Wills, *unpublished observations*).

Effects of Amiloride and Solution Osmolarity

In subsequent experiments, solution osmolarity was changed on only the serosal side and the mucosal osmolarity was held constant at 200 mOsm as before. To test whether the changes in I_{sc} and G_T were due to changes in the amiloride-sensitive conductance, the effects of 50 μM mucosal amiloride were tested in tissues bathed with serosal hyposmotic (170 mOsm), isosmotic (200 mOsm), and hyperosmotic (290 mOsm) solutions. The results are summarized in Table 1. In the absence of amiloride, G_T was significantly higher in the 170 mOsm solutions and lower in 290 mOsm solutions compared to the control (200 mOsm) solution (*see above*). However, in the presence of amiloride, the conductance values were reduced for 200 and 170 mOsm solutions and did not significantly differ between the groups. I_{sc} was zero for all groups in the presence of amiloride. No significant changes in G_T or I_{sc} were obtained for the 290 mOsm solution. Consequently, the amiloride-

Table 1. Solution osmolarity and effects of amiloride

	V_T (mV)	I_{sc} ($\mu A/cm^2$)	G_T ($\mu S/cm^2$)
200 mOsm			
Control	-18 ± 3	8 ± 1	453 ± 44
Amiloride	-1 ± 1^a	0 ± 0.4^a	349 ± 42^a
$n = 7$			
170 mOsm			
Control	-42 ± 4^b	22 ± 1^b	556 ± 42^b
Amiloride	0 ± 1^a	0 ± 0.2^a	330 ± 40^a
$n = 8$			
290 mOsm			
Control	-2 ± 1^b	0 ± 0.1^b	329 ± 36^b
Amiloride	-1 ± 1	0 ± 0.4	326 ± 35
$n = 4$			

[a] Paired t test: $P < 0.05$ compared to control.
[b] Unpaired t test: $P < 0.05$ compared to 200 mOsm.

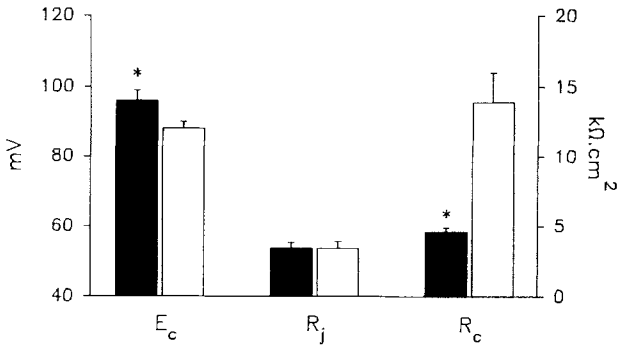

Fig. 4. Cellular resistance (R_c), driving force (E_c) and paracellular resistance (R_j) estimated from amiloride data and equivalent circuit analysis (paired measurements from eight epithelia)

sensitive conductance is decreased or abolished in hypertonic solutions and increased in hypotonic solutions.

In order to determine whether mucosal Na^+ entry plays a role in the effects of osmolarity, we reversed the order of solution replacement and amiloride addition in preliminary experiments. Tissues were first bathed in 200 mOsm solutions, next, treated with amiloride, and then exposed to a 170 mOsm serosal solution. No change was observed in I_{sc} or G_T as a result of the hyposmotic solution. However, following removal of amiloride from the mucosal bath, I_{sc} increased within 2–3 min to its usual value in 170 mOsm solutions ($I_{sc} = 22 \pm 3$ $\mu A/cm^2$). This increase was faster than the I_{sc} stimulation caused by hyposmotic solutions and was similar to the recovery of I_{sc} observed following amiloride removal. These findings indicate that the activation of the amiloride-sensitive current by serosal solution osmolarity is not dependent on Na^+ entry across the apical membrane.

Equivalent Circuit Analysis of Amiloride Effects

In previous studies (Wills & Millinoff, 1990), we determined that the amiloride-sensitive pathway could be described by the constant field equation and showed an essentially ohmic I-V relationship over a potential range of ± 100 mV. Therefore, alterations in the cellular driving force for Na^+ (E_c) or the cellular conductance (G_c) would be expected to result in proportional changes in I_{sc}.

As a first step in obtaining information about E_c and G_c, we used equivalent circuit analysis techniques to estimate E_c and to resolve the cellular resistance ($R_c = 1/G_c$) and the paracellular resistance (R_j). These values are compared for the 200 and 170 mOsm solutions in Fig. 4 ($n = 8$, paired measurements; estimates are not available for hyperosmotic solutions since the small or absent amiloride-sensitive currents for these conditions made this analysis impractical). R_j was not significantly different for hyposmotic and isosmotic solutions (3.4 ± 0.4 and 3.4 ± 0.5 $k\Omega cm^2$ for the 170 and 200 mOsm solutions, respectively). E_c averaged 88 ± 2 mV for the 200 mOsm solutions and was slightly higher (96 ± 3 mV, $P < 0.05$) in 170 mOsm solutions. This slight (~8%) increase in E_c, is too small to account for the nearly threefold increase in I_{sc} observed in this solution. In contrast, R_c was approximately three times lower for the 170 mOsm group ($R_c = 4.6 \pm 0.3$ and 14 ± 2 $k\Omega cm^2$ for 170 and 200 mOsm solutions, respectively). Consequently, the decrease in R_c is large enough to account for the observed increase in I_{sc}.

The Effects of Amiloride Concentration and Na : K Selectivity of the Amiloride-Sensitive Pathway in Isosmotic and Hyposmotic Solutions

Amiloride Dose Response

In a previous study, we characterized the amiloride dose-response relationship for the transepithelial conductance (G_t) in 170 mOsm solutions (Wills & Millinoff, 1990). The K_i for half-maximal inhibition of G_T was 0.7 ± 0.1 μM. In the present experiments, identical measurements were performed for four epithelia bathed in 200 mOsm solutions and K_i averaged 0.3 ± 0.1 μM. This value was in general agreement with our previous results.

Table 2. Solution osmolarity and the effects of amiloride in different mucosal solutions

	V_T (mV)	I_{sc} ($\mu A/cm^2$)	R_T ($k\Omega cm^2$)
200 mOsm			
Control (NaCl)	-21 ± 4	-9 ± 1	2.5 ± 0.4
Amiloride	1 ± 0.5^a	0 ± 0.3^a	3.1 ± 0.6^a
Control (KCl)	0 ± 0.1^b	0 ± 0.3^b	3.0 ± 0.8
Amiloride	1 ± 0.8	0 ± 0.3	3.1 ± 0.8
170 mOsm			
Control (NaCl)	-41 ± 7^c	-23 ± 3^c	1.8 ± 0.2^c
Amiloride	-1 ± 1^a	0 ± 0.2^a	3.4 ± 0.6^a
Control (KCl)	-1 ± 1^b	-1 ± 0.3^b	3.0 ± 0.4^b
Amiloride	0 ± 1^a	0 ± 0.2	3.3 ± 0.6^a

Paired measurements, $n = 4$. Serosal solution NaCl Ringer's.
[a] $P < 0.05$, compared to control.
[b] $P < 0.05$, compared to NaCl.
[c] $P < 0.05$ compared to 200 mOsm.

Macroscopic Na : K Selectivity

The Na : K selectivity ratio of the amiloride-sensitive pathway was also calculated by Wills and Millinoff (1990) from the amiloride-sensitive portion of the transepithelial conductance (G_{amil}). G_{amil} measured in normal (Na^+-containing) mucosal solutions was compared to G_{amil} measured in mucosal K^+ solutions, and the ratio of these values was used to estimate the macroscopic Na : K selectivity of the amiloride-sensitive conductance. In our previous study, this ratio averaged 15 ± 2 ($n = 8$) for 170 mOsm solutions, indicating a high Na : K selectivity.

Table 2 compares the effects of amiloride addition to mucosal Na^+ or K^+ solutions for 170 and 200 mOsm solutions. The results are paired measurements from four epithelia. For both solution osmolarities, there was little effect of amiloride on I_{sc} or R_T when the mucosal solution was replaced with KCl Ringer's solution. As in our previous study (Wills & Millinoff, 1990), the current-voltage relationship was essentially linear over a range of ± 100 mV for both mucosal Na^+ and K^+ solutions (*data not shown*). The ratio of G_{amil} values for Na^+ solutions compared to K^+ solutions averaged 15 ± 9 for the 200 mOsm solution, in reasonable agreement with our previous results. Consequently, solution osmolarities did not significantly alter the macroscopic Na : K selectivity of the amiloride-sensitive conductance.

Current Fluctuation Analysis of Osmotic Effects

A disadvantage of the above analysis is that it does not allow resolution of the apical and basolateral membrane components of E_c or R_c. To examine the amiloride-sensitive conductance at the membrane and single-channel level, we next turned to current fluctuation analysis techniques.

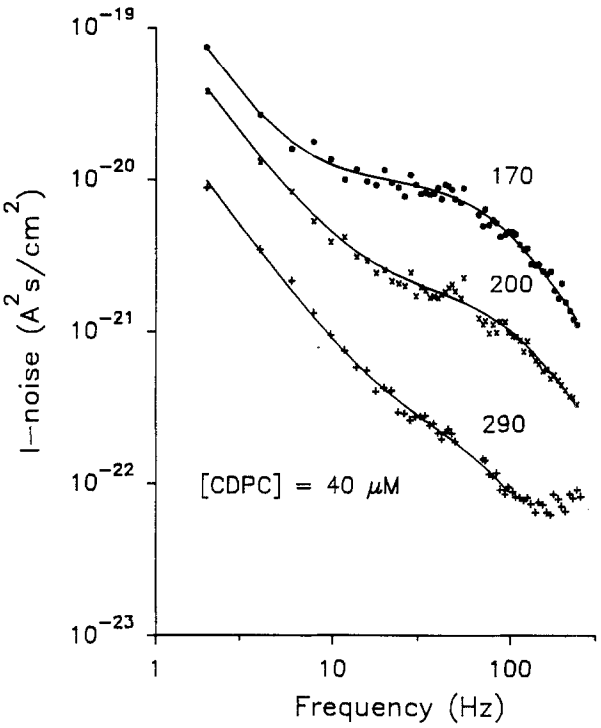

Fig. 5. Representative power-density spectra from a single tissue. The epithelium was bathed symmetrically with either 170 (●), 200 (×) or 290 (+) mOsm solutions. Smooth curves through the data points represent the results of computer-generated least-squares fits to Eq. (1). Results of the fits were as follows:

	B (A^2 sec/cm^2 $\times 10^{-19}$)	b	S_o (A^2 sec/cm^2 $\times 10^{-21}$)	f_c (Hz)	Residual error (%)
170 mOsm	2.3 ± 0.13	1.9 ± 0.04	9.7 ± 0.10	89 ± 1	0.2
200 mOsm	1.1 ± 0.03	1.6 ± 0.02	1.7 ± 0.02	111 ± 1	0.2

The best-fit parameters for the 290 mOsm solution spectra were $B = 0.3 \pm 0.1 \times 10^{-19}$, $b = 1.6 \pm 0.01$, $S_o = 0.2 \pm 0.003 \times 10^{-21}$ and $f_c = 78 \pm 10$ Hz; however, in other 290 mOsm experiments, the Lorentzian component was not detectable. I_{sc} for the three spectra averaged 23, 6, and 1 $\mu A/cm^2$, respectively

Figure 5 summarizes the results of a typical experiment. In this example, the epithelium was voltage clamped to 0 mV and the Na^+ channel blocker CDPC was present in the mucosal solution at a concentration of 40 μM. Data for power-density spectra are presented on a double-logarithmic plot of the amplitude of the current noise (ordinate) as a function of frequency in Hz (abscissa). The smooth curves through the data are the results of a computer-generated fit of the data by the sum of a Lorentzian function and a $1/f$ background noise component (*see* Materials and Methods).

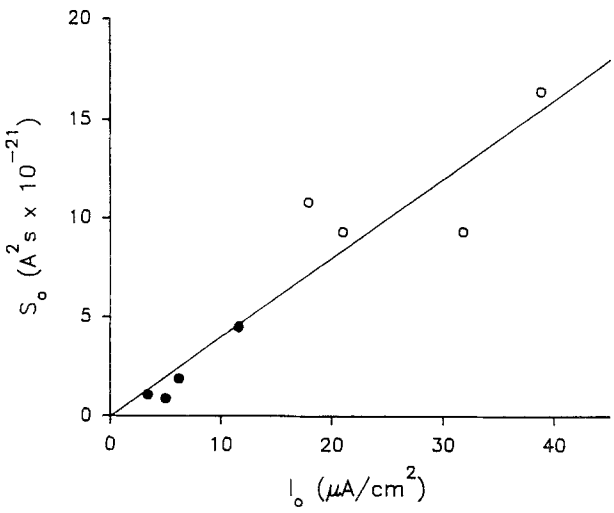

Fig. 6. Correlation between blocker-sensitive current (I_o) at 40 μM CDPC and the plateau value (S_o; normalized to 1 cm^2) for eight tissues. Filled circles = 200 mOsm bathing solutions; open circles = 170 mOsm solutions

Note that the spectra for both the 170 and 200 mOsm solutions showed distinct Lorentzian components with similar corner frequencies. In contrast, the plateau value (S_o) of the Lorentzian component was higher for the 170 mOsm solution compared to the 200 mOsm solution. The average plateau value for 40-μM CDPC and 170 mOsm solutions was 11.5 $\pm$ 1.1 $\times$ 10^{-21} A^2sec/cm^2 (n = 4 epithelia) compared to 2.1 $\pm$ 0.8 $\times$ 10^{-21} A^2sec/cm^2 for the 200 mOsm solution (n = 4 epithelia).

In contrast, spectra for the 290 mOsm solutions showed a lower overall noise amplitude than the spectra for other solutions. Although the data shown in Fig. 5 could be fitted to a Lorentzian function in most cases the spectra lacked this shoulder-shaped component. In other experiments, the voltage-clamp potential across the epithelium was increased to +45 mV at CDPC concentrations ranging from 10–100 μM. Again, no significant Lorentzian noise could be detected above the background noise. These findings suggest that the apical membrane channels are not conducting in the 290 mOsm solutions.

A shown in Fig. 6, a linear relationship was observed between the Lorentzian plateau value S_o and the remaining blocker-sensitive current I_o. This figure summarizes data from eight spectra at 40 μM CDPC. Open circles indicate 170 mOsm solutions and filled circles are 200 mOsm solutions. The linear relationship between these variables suggests that blocker kinetics and single-channel currents are constant for these two conditions and that the variability in I_o is directly correlated with a variation in channel number M. This deduction can be understood by considering that variability due to i would cause S_o to increase as a function of i^2, since $S_o = 4\tau i^2 MaP_oP_b$ (where $\tau = 1/2\pi f_c$, P_b is the probability that the channel is blocked and a is area; Wills & Zweifach, 1987). It is also apparent from this relationship that variability in I_o due to variations in blocker kinetics would be similarly complex (*see also* Eq. (5) below).

Calculation of Single-Channel Properties

Using a simple two-state model for CDPC blockage of the Na^+ channel (*cf.* Krattenmacher et al., 1988), we next calculated the kinetics of CDPC interaction with the channel for the 200 and 170 mOsm data. The rate constants for CDPC blockage (k_{on}) and unblockage (k_{off}) of the channel were initially calculated for each experiment from the linear relationship:

$$2\pi f_c = (k_{on})[\text{CDPC}] + k_{off} \quad (5)$$

where [CDPC] is the concentration of blocker (i.e., 10, 20, 40, 50 or 100 μM) and f_c, k_{on}, and k_{off} are defined as before. For 170 and 200 mOsm solutions, the rate constants were not significantly different (mean k_{on} = 4.4 $\pm$ 0.5 and 3.6 $\pm$ 0.6 μM^{-1} sec^{-1}, and mean k_{off} = 424 $\pm$ 18 and 469 $\pm$ 77 sec^{-1}, respectively; n = 4 for each solution).

Because the estimated kinetic parameters did not significantly differ, we next pooled the corner frequency data for the 170 and 200 mOsm solution conditions and analyzed mean f_c values for each blocker concentration using Eq. (5) above according to the methods of Krattenmacher et al. (1988) and Wills et al. (1984). These results are shown in Fig. 7. Kinetic parameters calculated from the mean data were k_{on} = 4.14 μM^{-1} sec^{-1} and k_{off} = 437 sec^{-1}, r^2 = 0.99.

Using the kinetic values above and data for S_o and blocker-sensitive currents (I_{Na}), we next calculated single-channel currents (i) using Eq. (2). As shown in Table 2, single-channel currents were similar for the 170 and 200 mOsm conditions. Helman and Baxendale (1990) reported that the number of open plus blocked channels increased as CDPC concentrations increased. However, such an increase was not reported by Krattenmacher et al. (1988) nor observed in the present study. Therefore, to calculate the number of conducting channels or channel density (M), we used a simple two-state model for CDPC blockage of Na^+ channels (*see* Eq. (3)) that was essentially identical to that used by Krattenmacher et al. (1988) rather than the more complex three-state model (Helman & Baxendale, 1990).

As shown in Table 3, M and I_{sc} were both ap-

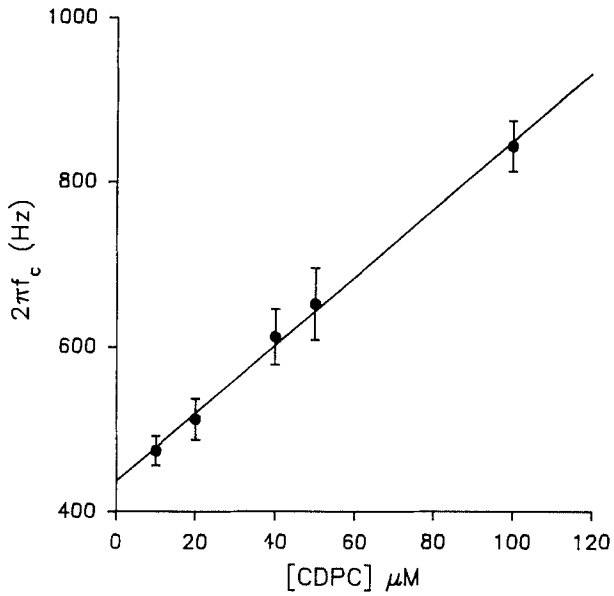

Fig. 7. Pooled corner frequency data from eight experiments showing mean and SEM for reaction rate ($2\pi f_c$) plotted against CDPC concentration. Linear regression of the data ($r^2 = 0.99$) was used to estimate k_{on} (slope = 4.13 ± 0.14 μM^{-1} sec^{-1}) and k_{off} (intercept = 437 ± 7 sec^{-1})

Table 3. Blocker kinetics and channel properties

Osmolarity (mOsm)	i (pA)	M ($10^6/cm^2$)	I_{sc} ($\mu A/cm^2$)
170 (n = 4)	0.2 ± 0.03	207 ± 53	29 ± 4
200 (n = 4)	0.2 ± 0.03	66 ± 16[a]	10 ± 3[a]

[a] $P < 0.05$ unpaired t test.

proximately threefold higher in 170 mOsm solutions than in 200 mOsm solutions. These results and the lack of detectable Na^+ channel noise in the 290 mOsm solution indicate that the number of conducting channels is increased in hyposmotic (170 mOsm) solutions and decreased in hyperosmotic (290 mOsm) solutions.

Discussion

The results of this study demonstrate a novel and potent regulation of Na^+ channel activity by serosal solution osmolarity. Thus, these findings confirm and extend to a single-channel level those originally observed by Ussing (1965) for the intact frog skin. Moreover, since the solution osmolarities used in this study are within the physiological range measured for amphibian plasma (Mayer, 1969), it is plausible that plasma osmolarity may be an important regulator of epithelial Na^+ transport.

Implications of the Slow Onset and the Sidedness of Effects

The slow onset of changes in transepithelial parameters in response to solution osmolarity changes suggests that this process is not due to a mechanical effect, such as cell stretching or shrinkage, but rather involves a slower process or cascade of events. Cell volume changes and mechanical activation of ionic channels are relatively fast events in epithelia. For example, Sackin (1987) found that stretch activation of K^+ channels in *Necturus* renal epithelial cells occurred within seconds after application of negative pressure. Similarly, Davis and Finn (1987) observed a rapid increase in cell volume in the frog urinary bladder that was maximal within 5 min following the application of serosal hyposmotic solutions. In contrast, ~20 min was required for the full effects of osmolarity on I_{sc}. This time course is slow enough to permit mediation of these effects by intracellular messengers and/or cytoskeletal events (*see below*).

Notably, the effects of anisosmotic solutions were observed for serosal, but not mucosal, solutions. This result indicates that the water permeability of the basolateral membrane is greater than that of the apical membrane. It is likely that movements of water across the basolateral membrane could result in events which affect the levels of intracellular messengers that regulate apical membrane Na^+ channel activity. Numerous intracellular messenger systems affect channels in epithelial membranes. For instance, increased intracellular cyclic AMP concentrations result in activation of apical membrane chloride channels in canine trachea (Welsh, 1988) and other secretory epithelia (*cf.* Wills & Zweifach, 1987). Factors that affect apical membrane Na^+ channels include G-binding proteins (Cantiello, Patenause & Ausiello, 1989; Eaton & Ling, 1989; Garty et al., 1989), intracellular Ca^{2+} levels (Garty & Asher, 1985), intracellular pH (Garty, Asher & Yeger, 1987; Palmer & Frindt, 1987), cAMP and protein phosphorylation/dephosphorylation (Sariban-Sohraby et al., 1988), and methylation (Sariban-Sohraby et al., 1984).

Site of Action of Osmolarity Effects

The effects on solution osmolarity on membrane ionic conductances have been studied in several epithelia (*cf.* Lewis & Donaldson, 1990). In general,

hypertonic solutions lead to cell shrinkage and decreases in basolateral membrane K^+ and/or Cl^- conductances. Conversely, hypotonic solutions result in cell swelling and increases in these conductances (e.g., Hazama & Okada, 1988).

In many tight epithelia, the apical membrane Na^+ conductance and the basolateral membrane K^+ conductance change in parallel, an unexplained phenomenon called "crosstalk" (Schultz, 1981; Diamond, 1982). In the A6 epithelium, the basolateral membrane conductance is largely due to potassium and is ~4 times higher than the apical membrane conductance (Wills & Millinoff, 1990). Consequently, the cellular driving force for Na^+ (E_c) largely reflects the sum of the basolateral membrane potential and the Na^+ chemical driving force across the ical membrane. For this reason, the changes in I_{sc} observed in the present study could have been mediated by a shift in the basolateral K^+ conductance (resulting in a change in E_c) and/or an alteration in the apical membrane Na^+ conductance.

In the present study only a slight (8% change) was noted in E_c in response to solution hyposmolarity. This change in the electrochemical driving force for Na^+ entry was too small to account for the large (~300%) increase in I_{sc}. In contrast, the increase in I_{sc} was accompanied by a nearly threefold reduction in the cellular resistance (R_c). The results of current fluctuation analysis measurements revealed that the number of conducting apical membrane Na^+ channels was similarly increased by approximately threefold.

In hyperosmotic solutions, I_{sc} was decreased or abolished and it was not possible to detect blocker-induced Na^+ channel noise. These findings were consistent with a reduction in the number of conductive channels. Because of the lack of detectable transepithelial currents under these conditions, it was not possible to assess other changes in E_c or the single-channel current.

Relationship to Cell Volume Changes

The effects of solution osmolarity on cell volume were not assessed in the present study. In recent preliminary measurements of cell height in A6 epithelia (Crowe & Wills, 1990), we have observed a different time course for cell height changes following exposure to anisosmotic solutions than that observed for I_{sc}. Cell height changed rapidly and typically reached steady state 5–10 min sooner than I_{sc}. Therefore, cell volume changes preceded osmolarity-induced alterations in Na^+ transport.

Blocker Kinetics and Single-Channel Properties

CDPC binding kinetics and single Na^+ channel properties were generally similar to those reported previously for other amphibian epithelia (*cf.* Wills & Zweifach, 1987). The apparent association rate constant (k_{on}) averaged ~4 μM^{-1} sec^{-1} and the dissociation rate constant (k_{off}) was ~400 sec^{-1} compared to previous values for k_{on} and k_{off} of ~4 μM^{-1} sec^{-1} and ~300 sec^{-1} observed by Krattenmacher et al. (1988) who used a similar protocol and a two-state model.

Single-channel currents were somewhat smaller in the present study and averaged 0.2 pA as compared to 1.0 pA reported for the frog colon (Krattenmacher et al., 1988) and 0.5 pA reported for the frog skin by Helman and Baxendale (1990). We have no explanation for this difference. However, membrane potentials in A6 cells are known to be lower than those of the frog skin (Thomas & Mintz, 1987).

Channel density (M) ranged between 60–200 million channels/cm^2 and was dependent on osmolarity conditions and the Na^+ transport rate (I_{sc} = 10–30 $\mu A/cm^2$). These values were also in reasonable agreement with previous measurements. M averaged ~30–60 million channels/cm^2 for I_{sc} values of ~20–30 $\mu A/cm^2$ in the study by Helman and Baxendale (1990); however, a somewhat lower value (~12 million channels/cm^2 for an I_{sc} of 33 $\mu A/cm^2$) was reported by Krattenmacher et al. (1988). Given the apparent differences in measurement conditions and tissues, the agreement between previous studies and the present results is reasonable.

Possible Mechanisms of Na^+ Channel Regulation

Conceivably, the differences in I_{sc} observed between the hyposmotic and control condition could be explained by the existence of more than one population of Na^+ channels and the recruitment of an additional population(s) at the lower osmotic strength. However, we could not detect differences in the amiloride or CDPC binding kinetics for these two conditions. Therefore, if two or more populations exist, their kinetic properties are similar or one population is predominate. In view of the lack of conducting Na^+ channels and low or absent I_{sc} observed under hyperosmotic conditions, it is parsimonious to suggest that a single-channel population and regulatory process may be responsible.

As discussed by Lewis and Donaldson (1990),

regulation of ionic channels can occur by three general mechanisms: activation, modulation or insertion. In the case of activation, as discussed previously, the slow time course of the osmolarity effects indicates that an intracellular messenger system might be involved. Recent studies by Cantiello et al. (1989) indicate that G-binding proteins, particularly the α_i-3 subunit are capable of activation of apical membrane Na^+ channels from A6 epithelia. However, to date, there are no known volume-activated G proteins. On the other hand, there have been numerous reports of cells with altered intracellular levels of cAMP (Watson, 1989), calcium (Wong, DeBell & Chase, 1990) and leukotrienes (*cf.* Hoffman & Simonsen, 1989) following exposure to anisosmotic solutions. Changes in the concentrations of intracellular regulators, such as pH (Palmer & Frindt, 1987) or calcium (Garty & Asher, 1985), or biochemical changes, such as phosphorylation or methylation of the channel or its regulatory peptides, could result in a shift in the channel open probability. As mentioned earlier, phosphorylation and methylation have been implicated in vasopressin and aldosterone activation of the channel, respectively (Sariban-Sohraby et al., 1984; 1988).

The second mode of channel regulation, channel modulation or modification, is unlikely since single-channel currents, blocker kinetics and the macroscopic Na : K selectivity were similar for the different osmotic conditions. On the other hand, the third means for channel regulation, insertion, is plausible and would involve increasing the number of conducting channels in the membrane by the direct insertion of channels or by fusion of channel-containing intracellular membrane vesicles. Vesicle fusion has been reported for apical membrane Na^+ channels of the mammalian urinary bladder (Lewis & deMoura, 1984) and for water channels in the amphibian urinary bladder (Wade, Stetson & Lewis, 1981). To examine this issue, we monitored net membrane area using the capacitance method of Lewis and deMoura (1984). Transepithelial capacitance (C_T) was measured before and after solution osmolarity changes and averaged 1.4 ± 0.1, 1.4 ± 0.1, and 1.4 ± 0.0 in 170, 200, and 290 mOsm solutions, respectively (n = 8). Consequently, if channels were inserted or withdrawn as the result of vesicle fusion or endocytosis, these changes did not result in a detectable change in net membrane area. Nonetheless, it is possible that anisosmotic solutions stimulate simultaneous (or parallel) processes of insertion of new channel-containing membrane and retrieval of existing plasma membrane. Experiments using extracellular fluid phase markers and cytoskeletal disruptive agents are now underway to determine whether membrane fusion and endocytosis play a role in these effects.

Possible Physiological Function

A potential problem for any study using a cell culture model system is whether the cells retain normal biochemical and physiological functions. Although we can only speculate as to the physiological function of an osmotically activated Na^+ transport regulatory mechanism, it is important to note that the A6 renal cell line (Rafferty, 1969) was originally derived from the kidney of the South African clawed toad, an aquatic species. An aquatic amphibian dehydrates quickly when kept away from moisture and can lose half its weight through evaporation of body fluids in a few hours (Heusser, 1968). Although, there are no available data concerning plasma osmolarity for *Xenopus laevis*, Mayer (1969) has reported values for *Rana esculenta* ranging from 210–260 mOsm, depending on whether the animal was maintained in distilled water or an 0.8% NaCl solution. Thus, it is possible that plasma osmolarity in *X. laevis* may vary across the range used in the present study. If Na^+ transport is indeed normally regulated by plasma osmolarity, an obvious advantage to such regulation is that the animal would increase Na^+ absorption at a time in which osmolytes are needed in the plasma and cease absorption when osmolyte values are already high.

Implications for Studies of Cultured Epithelia

Whether or not the effects of osmolarity reported in this study prove to be an important physiological modulator of epithelia Na^+ transport, the present findings have practical relevance for studies of cultured epithelia. Figure 8 compares the I_{sc} values from the present study to previous studies of A6 epithelium for which osmolarity data was reported. Although these studies tend to be clustered, there is excellent agreement between the previous studies and the present I_{sc} data. Therefore, it is possible that differences in solution or medium osmolarity may partly account for the large variability reported for Na^+ transport rates across A6 epithelia (*cf.* Wills & Millinoff, 1990). Interestingly, in preliminary experiments in which I_{sc} was stimulated by aldosterone or cAMP, I_{sc} showed a further increase when exposed to hyposmotic solutions. Therefore, it is tempting to speculate that osmolarity may modulate Na^+ transport by a mechanism that is independent of hormonal activation of the apical membrane Na^+ channels.

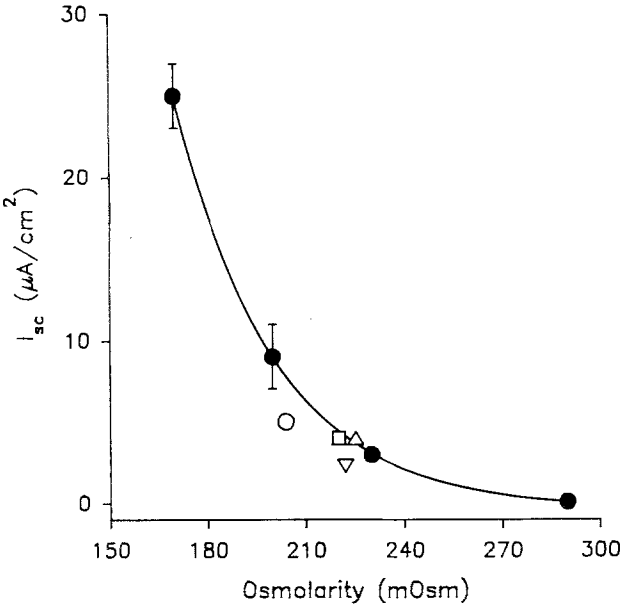

Fig. 8. Comparison of I_{sc} values from present study (filled circles) to previous values in literature for which osmolarity data was reported. Open circle = Fidelman et al. (1982), open square = Sariban-Sohraby, Burg and Turner (1983), open triangle = Keeler and Wong (1986), and inverted triangle = Thomas and Mintz (1987)

Conclusions

In summary, small (15%) decreases in serosal solution osmolarity resulted in a threefold stimulation of amiloride-sensitive I_{sc} in cultured renal (A6) epithelium. In contrast, $\geq$15% increases in osmolarity inhibited I_{sc}. The alterations in I_{sc} were accounted for by changes in the number of conducting Na^+ channels in the apical membrane. The time course of this regulation was slow with new steady-state levels usually attained within 30 min. Preliminary experiments suggest that this mode of Na^+ channel regulation may be independent of hormonal activation. Experiments are now underway to determine the precise mechanism and its possible physiological significance. An obvious biological advantage of such an osmotic regulation of Na^+ transport is that increased salt absorption would result during conditions of plasma hyposmolality and salt absorption would be decreased during dehydration (hyperosmolality).

The authors are indebted to Dr. Luis Reuss for his insightful suggestions and to Drs. Lewis and Donaldson for helpful discussions. This work was supported by N.I.H. grant DK-29962 to N.K.W.

References

Cantiello, H.F., Patenause, C.R., Ausiello, D.A. 1989. G protein subunit, α_i-3 activates a pertussis toxin-sensitive Na^+ channel from the epithelial cell line, A6. *J. Biol. Chem.* **264:**20867–20870

Crowe, W.C., Wills, N.K. 1990. Simultaneous monitoring of cell height and transepithelial Na^+ transport using fluorescence microscopy. *J. Am. Soc. Nephrol.* **1:**714

Davis, C.W., Finn, A.L. 1987. Interactions of sodium transport, cell volume, and calcium in frog urinary bladder. *J. Gen. Physiol.* **89:**687–702

Diamond, J.M. 1982. Transcellular cross-talk between epithelial membranes. *Nature* **300:**683–685

Eaton, D.C., Ling, B.N. 1989. The effect of cholera toxin (CTX), pertussis toxin (PTX) and GTPγS on highly selective Na^+ channels in A6 cells. *Proc. 22nd Annual Meeting American Society of Nephrologists.* (Washington, D.C.) p. 25A

Fidelman, M.L., May, J.M., Biber, T.U.L., Watlington, C.O. 1982. Insulin stimulation of Na^+ transport and glucose metabolism in cultured kidney cells. *Am. J.Physiol.* **242:**C121–C123

Garty, H., Asher, C. 1985. Ca^{++}-dependent temperature-sensitive regulation of Na^+ channels in tight epithelia. *J. Biol. Chem.* **260:**8330–8335

Garty, H., Asher, C., Yeger, O. 1987. Direct inhibition of epithelial Na^+ channels by a pH-dependent interaction with calcium, and by other divalent ions. *J. Membrane Biol.* **95:**151–162

Garty, H., Yeger, O., Yanovsky, A., Asher, C. 1989. Guanosine nucleotide-dependent activation of the amiloride-blockable Na^+ channel. *Am. J.Physiol.* **256:**F965–F969

Hazama, A. Okada, Y. 1988. Ca^{++} sensitivity of volume-regulatory K^+ and Cl^- channels in cultured human epithelial cells. *J. Physiol.* **402:**687–702

Helman, S.I., Baxendale, L.M. 1990. Blocker related changes of channel density: Analysis of a three state model for apical Na channels of frog skin. *J. Gen. Physiol.* **95:**647–678

Heusser, H.R. 1968. Frogs and toads. *In:* Animal Life Encyclopedia. Vol. 5: Fishes II and Amphibia. H.C.B. Grinek, editor. pp 365–366. Kindler—Verlaz, Zurich

Hoffman, E.K., Simonsen, L.O. 1989. Membrane mechanisms in volume and pH regulation in vertebrate cells. *Physiol. Rev.* **69:**315–382

Keeler, R., Wong, N.L.M. 1986. Evidence that prostaglandin E2 stimulates chloride secretion in cultured A6 renal epithelial cells. *Am. J. Physiol.* **250:**F511–F515

Krattenmacher, R., Fischer, H., Van Driessche, W., Clauss, W. 1988. Noise analysis of cAMP-stimulated Na current in frog colon. *Pfluegers Arch.* **412:**568–573

Lewis, S.A. 1977. A reinvestigation of the function of the mammalian urinary bladder. *Am. J. Physiol.* **232:**F187–F295

Lewis, S.A., deMoura, J.L.C. 1984. Apical membrane area of rabbit urinary bladder increases by fusion of intracellular vesicles: An electrophysiological study. *J. Membrane Biol.* **82:**123–136

Lewis, S.A., Donaldson, P. 1990. Ion channels and cell volume regulation: Chaos in an organized system. *News Physiol. Sci.* **5:**112–119

Marunaka, Y., Eaton, D.C. 1988. The effect of amiloride and an amiloride-analogue on single Na^+ channels from a renal cell line. *FASEB J.* **2:**A750

Mayer, N. 1969. Adaptation de *Rana esculenta* a des milieux varies. Etude speciale de L'excretion renale de l'eau et des

electrolytes au cours des changements de milieux. *Comp. Biochem. Physiol.* **29:**27–50

Palmer, L.G., Frindt, G. 1987. Effects of cell Ca and pH on Na channels from rat cortical collecting tubule. *Am. J. Physiol.* **253:**F333–F339

Perkins, F.M., Handler, J.S. 1981. Transport properties of toad kidney epithelia in culture. *Am. J. Physiol.* **241:**C154–C159

Rafferty, K.A. 1969. Mass culture of amphibian cells: Methods and observations concerning stability of cell type. *In*: Biology of Amphibian Tumors. M. Mizell, editor. pp 52–81. Springer—Verlag, New York

Sackin, H. 1987. Stretch-activated potassium channels in renal proximal tubule. *Am. J. Physiol.* **253:**F1253–F1262

Sariban-Sohraby, S., Burg, M.B., Turner, R.J. 1983. Apical sodium uptake in toad kidney epithelial cell line A6. *Am. J. Physiol.* **245:**C167–C171

Sariban-Sohraby, S., Burg, M., Wiesmann, W.P., Chiang, P.K., Johnson, J.P. 1984. Methylation increases sodium transport into A6 apical membrane vesicles: Possible mode of aldosterone action. *Science* **225:**745–746

Sariban-Sohraby, S., Sorscher, E.J., Brenner, B.M., Benos, D.J. 1988. Phosphorylation of a single subunit of the epithelial Na^+ channel protein following vasopressin treatment of A6 cells. *J. Biol. Chem.* **263:**13875–13879

Schultz, S.G. 1981. Homocellular regulating mechanisms in sodium-transporting epithelia: Avoidance of extinction by "flush-through." *Am. J. Physiol.* **241:**F579–F598

Thomas, S.R., Mintz, E. 1987. Time-dependent apical membrane K^+ and Na^+ selectivity in cultured kidney cells. *Am. J. Physiol.* **253:**C1–C6

Ussing, H.H. 1965. Relationship between osmotic reactions and active sodium transport in frog skin epithelium. *Acta Physiol. Scand.* **63:**141–155

Van Driessche, W., Lindemann, B. 1978. Low noise amplification of voltage and current fluctuations arising in epithelia. *Rev. Sci. Instrum.* **49:**52–57

Van Driessche, W., Zeiske, W. 1980. Spontaneous fluctuations of potassium channels in the apical membrane of frog skin. *J. Physiol.* **299:**1–16

Wade, J.B., Stetson, D.L., Lewis, S.A. 1981. ADH action: Evidence for a membrane shuttle action. *Ann. NY Acad. Sci.* **372:**106–117

Watson, P.A. 1989. Accumulation of cAMP and calcium in S49 mouse lymphoma cells following hyposmotic swelling. *J. Biol. Chem.* **264:**14735–14740

Welsh, M.J. 1988. Defective regulation of ion transport in cystic fibrosis airway epithelium. *In*: Cellular and Molecular Basis of Cystic Fibrosis. G. Mastella and P.M. Quinton, editors, pp. 321–344. San Francisco Press, San Francisco

Wills, N.K., Alles, W.P., Sandle, G.I., Binder, H.J. 1984. Apical membrane properties and amiloride binding kinetics of the human descending colon. *Am. J. Physiol.* **247:**G749–G757

Wills, N.K., Lewis, S.A., Eaton, D.C. 1979. Active and passive properties of rabbit descending colon: A microelectrode and nystatin study. *J. Membrane Biol.* **45:**81–108

Wills, N.K., Millinoff, L.P. 1990. Amiloride-sensitive Na^+ transport across culutured renal (A6) epithelium: Evidence for large currents and high Na:K selectivity. *Pfluegers Arch.* **416:**481–492

Wills, N.K., Zweifach, A. 1987. Recent advances in the characterization of epithelial ionic channels. *Biochim. Biophys. Acta* **906:**1–31

Wong, S.M.E., DeBell, M.C., Chase, H.S. 1990. Cell swelling increases intracellular free [Ca] in cultured toad bladder cells. *Am. J. Physiol.* **258:**F292–F296

Received 8 August 1990; revised 24 October 1990